UEQE #685568, VOL 00, ISS 00

Selection of Ground Motion Prediction Models for Seismic Hazard Analyzes in Zagros Region, Iran

MEHDI MOUSAVI, ANOOSHIRVAN ANSARI,
HAMID ZAFARANI, and ALIREZA AZARBAKHT

QUERY SHEET

This page lists questions we have about your paper. The numbers displayed at left can be found in the text of the paper for reference. In addition, please review your paper as a whole for correctness.

Q1: Au: Please provide shortened title for running head. 50 characters or less.
Q2: Au: Goodness test; Do you mean goodness-of-fit test here?
Q3: Au: Would 'addressed' be better here than 'issued'?
Q4: Au: Should this be weighting or weighing?
Q5: Au: Please provide a city/location for Budnitz et al., 1997.
Q6: Au: Please provide more information for Ghasemi et al., 2009.
Q7: Au: Please provide all author names instead of et al. for Zafarani *et al.*, 2011, 2012.
Q8: Au: Please provide all author names instead of et al. for Zafarani *et al.*, 2011, 2012.
Q9: Au: Please provide better quality figure for Figures 1–6.

TABLE OF CONTENTS LISTING

The table of contents for the journal will list your paper exactly as it appears below:

Journal of Earthquake Engineering, 00:1–24, 2012

ISSN: 1363-2469 print / 1559-808X online
DOI: 10.1080/13632469.2012.685568

Selection of Ground Motion Prediction Models for Seismic Hazard Analyzes in Zagros Region, Iran

MEHDI MOUSAVI, ANOOSHIRVAN ANSARI, HAMID ZAFARANI, and ALIREZA AZARBAKHT

Department of Civil Engineering, Arak University, Arak, Iran

The main objective of this article is to assess a set of candidate ground motion models in the Zagros region of Iran. The candidate models were chosen from three categories: local models that were developed based on the local data, regional models corresponding to Europe and Middle East data sets, and finally NGA (Next Generation Attenuation) models. Two different statistical approaches were applied for evaluation of these models, the first being the "likelihood" method, and the second the average "log-likelihood" method (LH and LLH). One of the most significant results of this study is that local ground motion models show more consistency with the recorded data than do NGA models.

Keywords Ground Motion Models; Evaluation of Fitness; Ranking; Zagros; Iran

1. Introduction

The selection of ground motion prediction models, and the determination of the contribution weight to assign to each of them, is a fundamental component of any seismic hazard analysis. It was demonstrated that the uncertainty corresponding to the selection of the attenuation model influences the hazard results more than other aspects of seismicity modeling [Toro 2006]. This epistemic uncertainty is often treated within the expert opinion approach through a logic tree framework [Budnitz *et al*., 1997]. The branch weights in a logic tree framework correspond to the degree of belief of experts in different prediction models. Although seemingly straightforward, the logic tree approach is a challenging tool to capture this uncertainty. Some professionals (e.g., Krinitzsky, 1995) believe that any attempt to assign numbers to degrees of belief, which are by nature personal and indefinable, and for which there are neither tests nor measurements, is a strategic mistake. From another point of view, it is indicated that due to the informal selection of the branch models and weights, the potential pitfalls regarding the construction and the use of logic trees is a rational expection [Bommer and Scherbaum, *et al*., 2008].

In addition to these general considerations, the absence of domestic experienced domestic experts is additional impediment with the use of logic trees in regions such as Iran. Because of these problems with "expert opinion" approaches we apply a recently developed statistically based scheme to assign the logic tree weights. The results can be used for seismic hazard studies in the Iran Zagros region, within a logic tree framework.

Received 10 November 2011; accepted 11 April 2012.
Address correspondence to Mehdi Mousavi, Department of Civil Engineering, Faculty of Engineering, Arak University, Arak, Iran. E-mail: m-mousavi@araku.ac.ir

2. Data Driven Ground Motion Model Selection

Given a set of data recorded in the real conditions of a specified region, how can one quantitatively judge different candidate ground motion models? This is the key question of any data-driven model selection. The statistical analysis of the residuals is the prime technique to distinguish the validity of these models. Because ground-motion models are commonly expressed in terms of logarithmic quantities, the residual is defined as the subtraction of the logarithmic-model predictions from the logarithms of the observed values, divided by the corresponding standard deviations of the logarithmic model:

$$\mathrm{r} = \frac{\log(SA_{obs}) - \log(SA_{pre})}{\sigma_{SA}}, \quad (1)$$

where $\mathrm{SA_{obs}}$ corresponds to the observed acceleration response spectra in a specified period, and $\mathrm{SA_{pre}}$ and σ_{SA} are the mean and the standard deviation of the predicted response spectra, respectively, using a given ground motion model. Ideally, the residual so defined is normally distributed with zero mean and unit variance. The fitness degree of the resulting residuals to this distribution defines the compatibility of the applied ground motion model with the recorded data. Statistical tests to measure the goodness of the issued fitness can be invoke, for example, the z-test can be used to test the hypothesis that the mean of residuals is zero [Montgomery *et al.*, 2003]. Also, the variance test may be used to test the residuals for unit variance [Montgomery *et al.*, 2003]. In order to test the shape of the residual distribution, it is convenient to perform a Lilliefors test of the default null hypothesis that the residuals sample comes from a normal distribution [Montgomery *et al.*, 2003]. These three tests in addition to a few other similar ones may be categorized as the traditional tests of residuals.

It is important to emphasize that most of the traditional tests only checks for one hypothesis, i.e. normal distribution, zero mean or unit standard deviation. As a consequence, they are not perfect tools for evaluation and ranking of the considered ground motion models. Due to this limitation, the likelihood-based measure (LH) recently emerged as another goodness test which is suitable for measuring not only the model fit, but also the underlying statistical assumptions [Scherbaum *et al.*, 2004]. One of the deficiencies of the above mentioned LH method is that it still requires a few subjective decisions, e.g., thresholds for acceptability. The dependency of the results on the sample size is another drawback of these methods. In order to overcome to these problems, a modern information-theoretic approach recently was proposed [Scherbaum *et al.*, 2009]. This method is more general than LH method and, in addition, does not depend on ad hoc assumptions e.g. size of samples and significant thresholds [Scherbaum *et al.*, 2009]. Q2

In this study, the information-theoretic approach in combination with the LH method and other goodness-of-fit measures are used to judge about the compatibility of the candidate ground motion models with the ground motion data recorded in the Zagros region, Iran. At first, a brief review of LH method, as well as information-theoretic approach is presented in the following sections.

3. The LH Method: An Efficient Tool for Ranking Ground Motion Models

The LH method was developed based on the concept of likelihood [Scherbaum *et al.*, 2004]. By recalling the normalized residual set defined in the former section, the LH can be defined corresponding to any observation, z_0, as:

$$LH(|z_0|) = \frac{2}{\sqrt{\pi}} \int_{\frac{|z_0|}{\sqrt{2}}}^{\infty} e^{-t^2} dt. \tag{2}$$

This equation defines a transform which maps any arbitrary residual distribution to another one. It was shown that the newer distribution is an indicator of the original distribution properties. For example, if the original distribution follows a perfect standard normal distribution with the zero mean and the unit variance, then the corresponding LH transform has a perfectly uniform distribution with median value equal to 0.5. Any deviation in the mean, standard deviation, and shape of the distribution of the residuals corresponds to a specified distribution, the median, and the standard deviation of LH values.

By using the LH distribution in combination with a few simple measures, Scherbaum *et al.* [2004] proposed a scheme to judge about the reliability of different ground motion models. The ground motion models are categorized into four classes according to this scheme:

- For a ground motion model to be ranked in the lowest accepted capability class (C), median LH value must be at least 0.2, an absolute value for the mean and the median of the normalized residuals, and their standard deviations must be less than 0.75. In addition, the normalized sample standard deviation is required to be less than 1.5.
- For a model to be ranked in the intermediate capability class (B), its median LH value must be at least 0.3, an absolute value of the mean and the median of the normalized residuals, and their standard deviations must be less than 0.5. In addition, their normalized sample standard deviation less than 1.25.
- For a model to be ranked in the highest capability class (A), its median LH value must be at least 0.4, the absolute value of both measures of the central tendency of the normalized residual distribution, and their standard deviations must not deviate by more than 0.25 from 0. In addition, their normalized sample standard deviation must be less than 1.125.
- A model that does not meet the criteria for any of these categories is ranked unacceptable, or class D.

More details about the LH method were issued in Sherbaum *et al.* [2004]. Q3

4. The Information-Theoretic: A Powerful Tool for Weighting the Models

One of the deficiencies of the above mentioned LH method is that it still requires a few subjective decisions, e.g.. thresholds for acceptability. The dependency of the results on the sample size is another drawback of these methods. In order to overcome to these problems, a modern information-theory approach recently was proposed [Scherbaum *et al.*, 2009]. This method is more general than the LH method and, in addition, does not depend on ad hoc assumptions, e.g., size of samples and significant thresholds [Scherbaum *et al.*, 2009].

The quantitative decision favoring different candidate models requires a meaningful measure to distinguish candidate probabilistic models. Within an information theory framework, this measure is given by the Kullback–Leibler distance [Delavaud *et al.*, 2009]. The Kullback–Leibler distance between two models *f* and *g* is presented as

$$\mathrm{D(f, g) = E_f\,(log_2\,(f)) - E_f\,(log_2(g))},$$

where E_f is the expected value taken with respect to f. This distance quantitatively represents the amount of information loss if the model f is substituted by model g. Here, for a base 2 logarithm, its unit is bit. For the model comparison (e.g., of two models g_1 and g_2), only their relative Kullback–Leibler distance, $D(f, g_1) - D(f, g_2)$, is taken into account. As a result, the expectation of the unknown model f drops out as a constant. The second expectation, $-E_f[\log_2(g)] = -\int_{-\infty}^{+\infty} f(x)\log_2 g(x)$, can be estimated by the average sample log likelihood:

$$\mathrm{LLH} := -\frac{1}{N}\sum_{i=1}^{N}\log_2(g(x_i)). \tag{3}$$

This latter estimator, LLH, is used as ranking criterion in an information theory framework. By using the LLH values, it is possible to assign correct weights to K given attenuation models [Scherbaum *et al* 2009]:

$$w_j = \frac{2^{-\log_2(LLH_j)}}{\sum_{j=1}^{K} 2^{-\log_2(LLH_j)}}. \tag{4}$$

In this study, the LH method was applied to rank ground motion models into four classes: A, B, C, and D. By excluding the models categorized as D, the information-theory method was used to assign appropriate weights to the remained models.

5. The Testing Ground Motion Dataset

In order to test the effectiveness of candidate ground motion models, 21 significant earthquakes were chosen from the Zagros region of Iran, each with moment magnitude between 5.0–6.2. Five significant events from East-Central Iran region were added to the testing dataset due to the inadequate magnitude range of recorded ground motions in the target region. This inclusion is considered valid since some previous studies showed a general similarity between the two regions [Hassani *et al.,* 2011; Zaferani *et al.*, 2012].

The enriched combined dataset covers magnitudes in range 5.0–7.2 that is sufficient for convenient probabilistic seismic hazard analyzes taking to account the lack of historical earthquakes greater than M7.4 in the Zagros region [Ambraseys and Melville, 1982]. Table 1 shows the information about each of the events with the corresponding reference. A total of 114 records were extracted from the website of the Building and Housing Research Center (BHRC) in Iran. Data was selected so that the validity range for the source to site distance was respected for all ground motion models. This means that sites farther than 100 km or closer than 4 km in epicentral distance were excluded. Also, to avoid uncertainties regarding site conditions, only records where average S-wave velocities in the upper 30 m (V_{S30}) are known for the corresponding stations were chosen. The name, code number, epicentral distance, and V_{S30} of these stations are listed in Table 2. The uncorrected acceleration time series recorded by a given station were corrected for the instrument response and baseline, following a standard algorithm [Trifunac and Lee, 1973]. Multi-resolution wavelet analysis [Ansari *et al.*, 2010] was performed to remove undesirable noise from the recorded signals.

Figure 1 shows the magnitude-distance distribution of the employed ground motion records. The different stations are categorized into three different soil classes: rock for $V_{S30} > 750$ m/s, stiff soil for 375 m/s $< V_{S30} < 750$ m/s, and soft soil for $V_{S30} < 275$ m/s,

TABLE 1 Paramaeters for the Zagros earthquakes used in this study

No.	Event date	Time	Mw	Depth (km)	§N	Reference of Mw
*1	1979/11/27	15:36	7.1	10	4	HRVD
*2	1997/05/10	07:57	7.2	13	3	HRVD
*3	1998/03/14	19:40	6.6	5	2	HRVD
4	1999/08/21	05:31	5.0	25	3	HRVD
5	1999/05/06	23:00	6.2	7	5	HRVD
6	1999/05/06	23:13	5.7	10	3	HRVD
7	1999/10/31	15:09	5.2	15	4	HRVD
8	2002/04/24	19:48	5.4	25	6	HRVD
9	2002/12/24	17:03	5.2	20	6	HRVD
10	2003/07/10	17:06	5.8	10	4	HRVD
11	2003/07/10	17:40	5.7	15	4	HRVD
12	2003/11/28	23:19	5.0	25	3	HRVD
*13	2003/12/26	01:56	6.5	3	3	HRVD
*14	2005/02/22	02:25	6.3	10	6	HRVD
15	2005/11/27	10:22	5.9	12	6	HRVD
16	2006/03/30	19:36	5.1	20	8	HRVD
17	2006/03/31	01:17	6.1	12	9	HRVD
18	2006/03/31	11:54	5.1	26	6	HRVD
19	2006/06/28	21:02	5.8	12	4	HRVD
20	2008/05/05	21:57	5.2	12	3	HRVD
21	2008/09/10	11:00	6.1	12	5	HRVD
22	2008/09/11	02:16	5.2	7	3	HRVD
23	2008/09/17	17:43	5.2	12	3	HRVD
24	2008/12/07	13:36	5.4	12	4	HRVD
25	2008/12/08	14:41	5.1	12	3	HRVD
26	2008/12/09	15:09	5.0	14	3	HRVD

*Selected from East-Central Iran; §N, Number of used records; HRVD: Harvard seismology.

as shown in Fig. 1. The site classifications used in the models considered are not identical; nevertheless, the comparisons are made for comparable site classes.

Due to paucity of data, as shown in Fig. 1, the testing process does not include events with Mw $>$ 6.5 and R $<$ 50 km.

The candidate ground motion models are firstly introduced in the following section and then the fitness of them for the gathered dataset is analyzed.

6. Candidate Ground Motion Attenuation Models

Based on different studies on the seismotectonic characteristics of Iran, it was shown that all of the Iranian plateau earthquakes are shallow, intra-plate events [Berberian 1976]. Also, a general similarity is reported between the shallow intra-plates events from different regions, including Turkey and California [Chen and Atkinson 2002]. According to these criteria, candidate ground motion models were selected from three categories:

- Ground motion models developed specially for the region of Iran (Category 1)
- Ground motion models developed for the Mideast-Europe region (Category 2)
- Global ground motion models developed by the "Next Generation of Ground-Motion Attenuation Models" (NGA) project (Category 3)

TABLE 2 Observed data from the Zagros and East-Central Iran regions

Mw	Code	Station name	Epi. distance (km)	Vs30 (m/s)
7.1	1142-1	Gonabad	94	529
7.1	1139	Ghaen	53	889
7.1	1140	Khezri	76	701
7.1	1138-1	Sedeh	90	1180
7.2	1750-2	Marak	105	872
7.2	1770	Mussaviyeh	105	848
7.2	1753	Sangan	80	941
6.6	1864-1	Abaraq	90	641
6.6	1866	Baqein	76	516
5	2251	Noor abad	36	758
5	2183/01	Boroujerd	69	579
5	2196/02	Aleshtar	47	621
6.2	2126/03	Ghaemiyeh	48	617
6.2	2121/02	Kazeroon	28	352
6.2	2131/02	Balaadeh	29	1380
6.2	2123/02	Gooyom	56	598
6.2	2130/01	Khan zeynioun	26	773
5.7	2131/03	Balaadeh	18	1380
5.7	2123/03	Gooyom	64	598
5.7	2130/02	Khan zeynioun	36	773
5.2	2216/01	Kazeroon	36	352
5.2	2217	Romghan	34	1362
5.2	2218/03	Ghaemiyeh	60	617
5.2	2219/12	Balaadeh	19	1380
5.4	2706/02	Armanijan	25	390
5.4	2707/02	Aran	58	175
5.4	2708/02	Bistoon	35	750
5.4	2710/02	Sahneh	39	375
5.4	2711/02	Sonqor	37	1477
5.4	2747/02	Lenj Ab	40	375
5.2	2933/03	Armanijan	24	390
5.2	2934	Aran	48	175
5.2	2935	Bistoon	28	750
5.2	2936/01	Sahneh	29	375
5.2	2937/01	Sonqor	34	1477
5.2	2999/01	Lenj Ab	44	375
5.8	3040/01	Hajiabad-3	27	561
5.8	3041/01	Jouyom	21	1244
5.8	3042/01	Zahedshahr	60	390
5.8	3045/01	Jahrom	64	375
5.7	3040/03	Hajiabad-3	38	561
5.7	3041/02	Jouyom	18	1244
5.7	3042/02	Zahedshahr	63	390
5.7	3045/02	Jahrom	61	375
5	3134/02	Hajiabad-3	44	561

(*Continued*)

TABLE 2 (Continued)

Mw	Code	Station name	Epi. distance (km)	Vs30 (m/s)
5	3135	Jouyom	27	1244
5	3136/05	Doobaran	30	1363
6.5	3168/002	Bam	4	499
6.5	3170/002	Jiroft	74	343
6.5	3162/001	Mohamadabad	49	507
6.3	3660/001	Chatrud	27	852
6.3	3702	Davaran	57	752
6.3	3679	Deh-e-Loulo	61	617
6.3	3688	Horjand	42	999
6.3	3661	Ravar	55	853
6.3	3671/001	Zarand	19	226
5.9	3912	Bandar-e-Abas 1	62	337
5.9	3917	Bandar-e-Abas 2	62	375
5.9	3913	Bandar-e-Khamir	39	679
5.9	3910	Kahoorestan	61	807
5.9	3909	Qeshm	45	757
5.9	3915/01	Suza	21	1334
5.1	4027/005	Chalan choolan	24	428
5.1	4023/002	Boroujerd	34	579
5.1	4022/001	Dorood	37	771
5.1	4019/001	Khoram abad 1	47	375
5.1	4018/002	Chaghalvandi	29	616
5.1	4055/002	Shool Abad	67	1084
5.1	4035/002	Tooshk-e-Ab-e-Sar	31	891
5.1	4052/002	Darreh-Asbar	40	935
6.1	4018/03	Chaghalvandi	35	616
6.1	4019/02	Khoram Abad	54	375
6.1	4022/02	Dorood	23	771
6.1	4025	Aleshtar	67	621
6.1	4027/08	Chalan Choolan	13	428
6.1	4052/03	Darreh-Asbar	67	935
6.1	4024	Noor Abad	101	758
6.1	4055/03	Shool Abad	56	1084
6.1	4035/03	Tooshk-e-Ab-e-Sar	38	891
5.1	4136	Khoram Abad	52	375
5.1	4055/004	Shool Abad	78	1084
5.1	4035/006	Tooshk-e-Ab-e-Sar	31	891
5.1	4032	Dorood	47	771
5.1	4034	Boroujerd	32	579
5.1	4044	Chaghalvandi	33	616
5.8	4147/13	Tomban	13	778
5.8	4152	Bandar-e-Khamir	33	679
5.8	4128	Qeshm	52	757
5.8	4144	Bandar-e-Abas 2	68	375
5.2	4573	Doobaran	33	1363

(*Continued*)

TABLE 2 (Continued)

Mw	Code	Station name	Epi. distance (km)	Vs30 (m/s)
5.2	4574	Jouyom	14	1244
5.2	4575	Zahedshahr	65	390
6.1	4672	Bandar-e-Khamir	38	679
6.1	4686/003	Tomban	23	778
6.1	4678/001	Suza	40	1334
6.1	4675/001	Tabl	17	931
6.1	4676	Kahoorestan	66	807
5.2	4675/002	Tabl	22	931
5.2	4678/005	Suza	47	1334
5.2	4686/019	Tomban	30	778
5.2	4687/001	Bandar-e-Abas 1	60	337
5.2	4690/001	Suza	17	1334
5.2	4688/001	Qeshm	41	757
5.4	4732/002	Suza	35	1334
5.4	4735	Tabl	14	931
5.4	4734	Bandar-e-Abas 1	70	337
5.4	4736	Bandar-e-Khamir	25	679
5.1	4742	Bandar-e-Abas 1	68	337
5.1	4739/001	Suza	33	1334
5.1	4741/001	Tabl	15	931
5.1	4737/001	Qeshm	54	757
5	4739/002	Suza	30	1334
5	4737/002	Qeshm	55	757
5	4741/002	Tabl	16	931

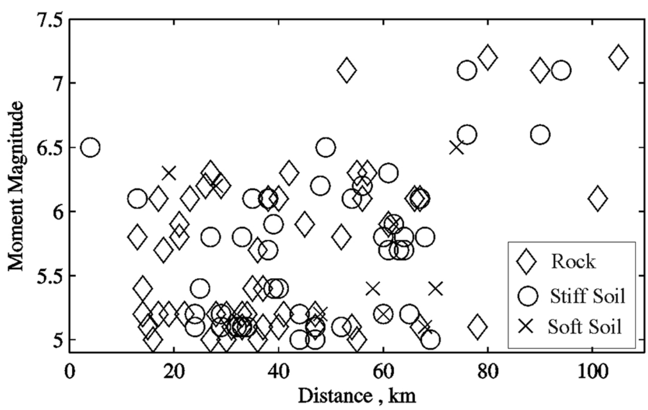

Q9

FIGURE 1 The magnitude – distance distribution of the observed data used in this study.

The Next Generation Attenuation (NGA) project has developed a series of ground motion models intended for application to geographically diverse regions; the only constraint is that the region be tectonically active with earthquakes occurring in the shallow crust. Five sets of ground-motion models were developed by teams working independently 175 but interacting with one another throughout the development process. According to Power *et al* [2008], each development team was required to use a subset of the database developed during the NGA project and supporting information in the database (e.g., source parameters, source-to-site distance, and local site condition of the recording station). The database used to develop the NGA GMPEs is large (i.e., 3551 recordings from 173 earthquakes). From this common database, individual records could be selected or excluded at the discretion of each team. According to Abrahamson *et al* [2008], an important issue in the selection of the earthquakes was the applicability of the well-recorded large-magnitude earthquakes from outside of the Western United States (1999 Chi-Chi and 1999 Kocaeli) to the prediction of ground motions in the WUS. All of the developers considered both the Chi-Chi and Kocaeli data to be applicable to the WUS. The data selection criteria and resulting data sets used by each developer are summarized in the developers' articles in a special issue of *Earthquake Spectra* (2008). Here, the NGA models of Boore and Atkinson [2008], Campbell and Bozorgnia, [2008], Chiou and Youngs [2008], and Abrahamson and Silva [2008], are compared with the Iranian strong-motion database.

Ground motion models were selected according to the criteria proposed recently by Bommer *et al* [2010]. Two significant points were particularly considered.

- Models that were superseded by a more recent publication were avoided.
- Models that lack either nonlinear magnitude dependence or magnitude-dependent decay with distance were excluded. This criterion was recommended in some of recent studies (e.g., Cotton *et al*., 2008; Bommer *et al*., 2010). This item should be met just by empirically developed models, not by finite source stochastic models.

Finally, it should be noted that epistemic uncertainties may be influenced by different measures of distance and magnitude. Different attenuation relationships use different forms of distance measures (such as R_{epi}, R_{hypo}, R_{rup}, R_{jb}, etc.) and magnitude scales (Ms, mb, Mw, etc.) for prediction of ground motion parameters. Here, to avoid any inconsistencies caused by magnitude conversion formulas we restricted the dataset only to events with available moment magnitude. Also, we considered the attenuation equations which are based on the moment magnitude scale.

Here, the selected ground motion models are briefly described.

(1) Zafarani *et al*. [2011] [Zetal11]: Using the Specific Barrier Model (SBM), a finite source stochastic model was proposed by Zafarani *et al*. [2011] to be used in The Zagros region. The recorded ground motions in The Zagros region have an upper bound of magnitude 6.2. So, due to the paucity of data for large earthquakes, the applicability of derived empirical ground motion models is limited to small and medium events. However, where a stochastic model can be calibrated, the valid range of achieved model can be extended to a wider range of magnitude. Zetal11 model covers magnitudes Mw4.4 to 7.5. From the ground motion records used in this study, records from earthquakes with magnitude lower than 6.25 were applied in the development of Zetal11.

(2) Ghasemi *et al*. [2009] [Getal09]: They processed the Iranian dataset to find the ground motion model for 5%-damped horizontal spectral acceleration. Also, in order to achieve a wider range of magnitude and distance, the selected West-Eurasian records were added to the Iranian dataset.

(3) Sharma *et al*. [2009] [Setal09]: This model was driven to be applied for the Indian Himalaya. However, due to a lack of data from India, additional strong-motion data

were included from the Zagros region of Iran, which has comparable seismotectonics to the Himalaya.

(4) Akkar and Cagnan [2010] [AC10]: They proposed this model for estimating peak horizontal acceleration, velocity, and pseudospectral acceleration using the recently compiled Turkish ground-motion database

(5) Akkar and Bommer [2010] [AB10]: A wide range of ground motion data from Europe and the Middle East was applied to develop the AB10 model.

(6) Kalkan and Gulkan [2004] [KG04]: A data set created from a suite of 112 strong ground motion records from 57 earthquakes were used by Kalkan and Gulkan to develop attenuation relationships for Turkey.

(7) Abrahamson and Silva [2008] [AS08]: The model is applicable to magnitudes 5–8.5, distances 0–200 km, and spectral periods of 0–10 s. In place of generic site categories (soil and rock), the site is parameterized by average shear-wave velocity in the top 30 m (VS30) and the depth to engineering rock (depth to VS = 1000 m/s). An additional source parameter, depth to the top of rupture, is also included.

(8) Boore and Atkinson [2008] [BA08]: The main predictor variables in BA08 are moment magnitude M, closest horizontal distance to the surface projection of the fault plane RJB, and the time-averaged shear-wave velocity from the surface to 30 m VS30. The equations are applicable for M = 5–8, Rjb < 200 km, and VS30 = 180–1300 m/s.

(9) Campell and Bozorgnia [2008] [CB08]: They used a subset of the PEER NGA database and excluded recordings and earthquakes that were believed to be inappropriate for estimating free-field ground motions from shallow earthquake mainshocks in active tectonic regimes. The resulting equations are valid for magnitudes ranging from 4.0 up to 7.5–8.5 (depending on fault mechanism) and distances ranging from 0–200 km. The model explicitly includes the effects of magnitude saturation, magnitude-dependent attenuation, style of faulting, rupture depth, hanging-wall geometry, linear and nonlinear site response, 3-D basin response, and inter-event and intra-event variability.

(10) Chiou and Youngs [2008] [CY08]: They limited the data to recordings within 70 km of the earthquake rupture in order to remove the effects of bias in the strong motion data sample. This limitation results in a total data set of 1950 recordings from 125 earthquakes. The model incorporates improved magnitude and distance scaling forms as well as hanging-wall effects. Site effects are represented by smooth functions of average shear wave velocity of the upper 30 m (VS30) and sediment depth. A key difference in the data sets is the treatment of aftershocks. The AS08 and CY08 data sets include aftershocks, resulting in a much larger number of earthquakes than the BA08 and CB08 sets [Abrahamson *et al.*, 2008].

The above listed attenuation models are summarized in Table 3. The valid range of magnitude and distance for these models is indicated in this table.

Figure 2 compares the selected ground motion models for the scenario Mw5.8 and R = 45km. This scenario corresponds to the average magnitude and distance of the used dataset, strike slip faulting mechanism, and shear wave velocity 750 m/s.

Regarding the additional parameters needed to be used for the selected attenuation equations, the general strategy was to constrain the input parameters as much as possible using the local data and sources where this is available and if not, using reasonable arguments and previous experiences elsewhere to adopt the best plausible set of input parameters. In the absence of exact data, a generic dip angle of 45° was assumed for reverse faults in the Zagros region based on Berberian [1995]. For some of the larger events (e.g.,

TABLE 3 Candidate ground motion models

No	Model	Abb.	Dominant region	Category	Mw	Distance
1	Zafarani *et al.* [2011]	Zetal11	Iran	1	4.4–7.5	2–200 km
2	Ghasemi *et al.* [2009]	Getal09	Iran	1	5.0–7.4	5–500 km
3	Sharma *et al.* [2009]	Setal09	India, Iran	2	5.0–7.0	0–200 km
4	Akkarand Cagnan [2010]	AC10	Turkey	2	3.5–7.6	0–200 km
5	Akkar & Bommer [2010]	AB10	Europe, Middle east	2	5.0–7.6	0–100 km
6	Kalkan and Gulkan [2004]	KG04	Turkey	3	4.0–7.4	1–200 km
7	Abrahamson and Silva [2008]	AS08	California	3	5.0–8.5	0–200 km
8	Boore and Atkinson [2008]	BA08	California	3	5.0–8.0	0–200 km
9	Campbell and Bozorgn [2008]	CB08	California	3	4.0–7.5	0–200 km
10	Chiouand and Youngs [2008]	CY08	California	3	4.2–7.9	0–∼100 km

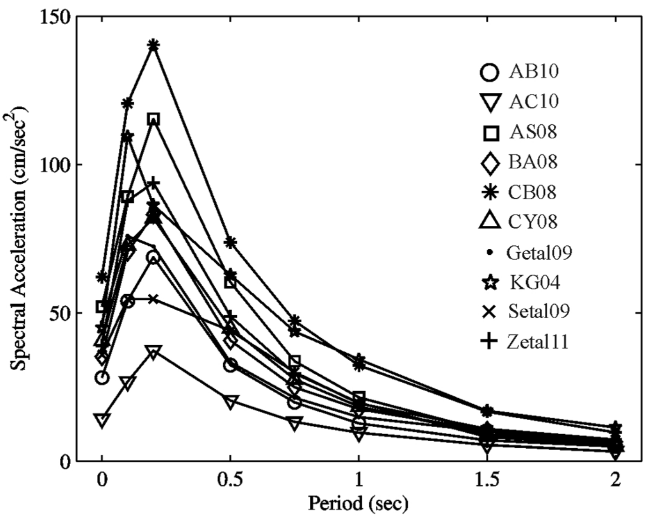

Q9

FIGURE 2 Comparison of spectral acceleration of different ground motion models for scenario Mw5.8 and R = 45 km, strike slip faulting mechanism, and shear wave velocity 750 m/s.

the catastrophic 2003 Mw 6.5 Bam earthquake) there is exact information about the fault plane and source geometry (see, e.g., Table 1 in Zafarani *et al.*, 2008). Regional values of Ztor were adopted from crustal velocity studies in the region (e.g., Hatzfeld *et al.* 2003). The Joyner-Boore distance and the rupture distance were calculated for recorded ground motions.

7. Ranking of the Ground Motion Models by Analysis of Residuals

For each of the ground motion records described in Table 2, synthetic acceleration response spectra, $S_a(T)$, were generated using the 10 candidate ground motion prediction models presented in Table 3 over 7 periods including (0.1 s, 0.2 s, 0.5 s, 0.75 s, 1.0 s, 1.5 s, and 2 s) and the peak ground acceleration (PGA). By using Eq. (1), the residual set associated by each model is achievable for any arbitrary period. As an example, the residual distribution of $S_a(T = 1.0\text{ s})$ is shown in Fig. 3 for all of ground motion models. The standard normal distribution, as the ideal distribution of the residuals, is also plotted for each case in Fig. 3.

Here, three statistical analyzes are applied to gain an insight into the goodness of a standard normal distribution to the residuals. Due to the space limitations, only results of the statistical analysis for $S_a(T = 1.0\text{ s})$ are explained here.

7.1. The z-test

The null hypothesis is that the mean of the normalized residual set is zero. The residuals are assumed to be gained from a normal distribution of known variance (unit). The p-value indicates the smallest level of significance that would lead to rejection of the null hypothesis with the given data. A small p-value means that the difference between the estimated mean and the model mean is significant and thus it is very unlikely that the observations were produced by the candidate model. On the other hand, a large p-value enhances our confidence in the model [Scherbaum *et al.*, 2004]. Table 4 includes the z-test p-values for different ground motion models for residual distribution of $S_a(T = 1.0\text{ s})$. According to this table, the null hypothesis can be rejected for the majority of the given models.

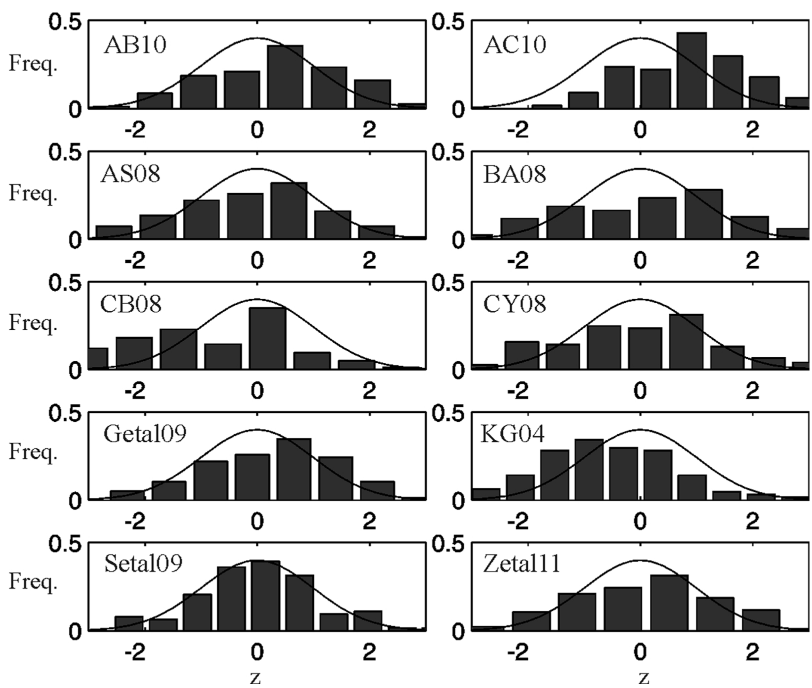

Q9

FIGURE 3 Residual distribution of $S_a(T = 1.0\text{ s})$ with respect to different ground-motion models. Solid line shows the expected distribution function for a standard normal distribution.

TABLE 4 Traditional tests p-values; T = 1.0 s

Model name	z-test	lil-test
AB10	0.00	0.500
AC10	0.00	0.500
AS08	0.40	0.346
BA08	0.150	0.298
CB08	0.00	0.063
CY08	0.81	0.26
Getal09	0.00	0.500
KG04	0.00	0.500
Setal09	0.81	0.500
Zetal11	0.10	0.500

7.2. The Lilliefors Test

The Lilliefors test was used to test the null hypothesis that data come from a normally distributed population, when the null hypothesis does not specify the mean and variance of the distribution. Table 4 includes the Lilliefors test p-values for different ground motion models for residual distribution of $S_a(T = 1.0\text{ s})$. According to this table, there is not enough evidence to reject the null hypothesis for any of models.

As shown in Table 4, there is imperfect correlation between the results of two employed tests for all models. For example, according to the z-test, the difference between the estimated mean and the Getal09 mean is significant, whereas the higher p-value of Lilliefors test confirms a normal distribution of the residuals. Therefore, as also mentioned earlier, the traditional tests are not perfect tools for evaluation and ranking of the models [Scherbaum *et al.*, 2004]. Perhaps the only inference to be gained from the above table is that the model CB08 shows weaker performance compared to the others, because both p-values are small.

7.3. The LH test

The distribution of LH values for $S_a(T = 1.0\text{ s})$ are shown in Fig. 4. The distribution of LH values, as seen in Fig. 5, is more near to a uniform shape in some cases, e.g., Setal09 than in some other cases, e.g., CB08. The statistical measurements of LH values are shown in Table 5, as well as some other measurements of the residuals for acceleration response spectra in period T = 1.0 s, $S_a(T = 1.0\text{ s})$.

The goodness-of-fit measures in this method are: the median LH values (MEDLH) and the median, mean, and the standard deviation of the normalized residuals (MEDNR, MEANNR, and STDNR, respectively). The corresponding standard deviations of these measures (σ) are calculated using the bootstrap technique through data re-sampling [Efron and Tibshirani, 1993]. By using these measures and based on the scheme presented in the former sections, the ground motion models are ranked in the categories A, B, C, or D in the last column.

The earlier table may be repeated for the different periods. The relative similarity of ranking results for different periods may be interpreted as a sign of method stability. This hypothesis is studied through Table 6, which shows LH based ranking of models in different periods.

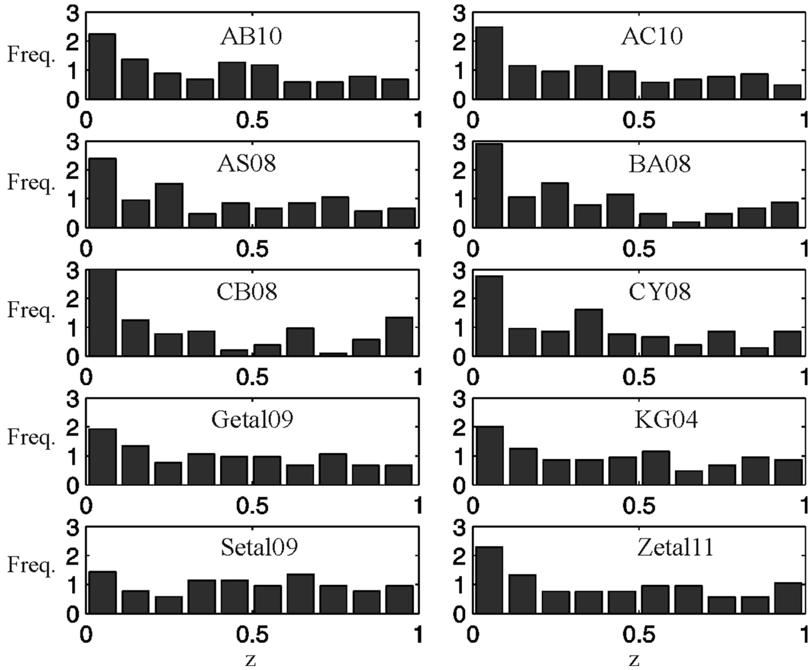

Q9

FIGURE 4 Distribution of LH values for Sa(T = 1.0 s) with respect to different ground-motion models.

Inspection of the last two tables shows that three models: Setal09, Zetal11, and Getal09 are ranked A or B for all periods. Another finding is that two models, CB08 and AC10, are always assigned D, or unacceptable.

Since the ranking results are more or less stable for the different periods, it was decided to merge all residuals into a unit set and then repeat the ranking procedure. Table 7 shows the ranking of models based on this united residuals set. Table 7 can be accounted as the final ranking of models based on LH method. According to this ranking, two models, CB08 and AC10, should be excluded from the acceptable models. An interesting result of this table is that all models developed specially for Iran region (Category 1) are ranked B, and the NGA models (Category 3) are ranked C and D. On the other hand, models that were categorized as Europe and Middle East models (Category 2) show a wide range of performance, from B–D.

As shown in Fig. 1, the ground motion database used is dominantly influenced by small and medium events. This issue may influence the above conclusions, which favor the use of local models compared to NGA models. In order to study this problem, Tables 8 and 9 were prepared in respect to the ground motions with Mw $>$ 6.25 and Mw $<$ 6.26, respectively.

Two local models, Zetal11 and Getal09, are located in the top level of Tables 7, 8, and 9. This issue again confirms the improved performance of local models compared with NGA models.

We next exclude CB08 and AC10 from the usable models, and study the ranking of the remaining models using the information-theory method. The agreement of the two thus-obtained rankings provide an estimate of the reliability of the results.

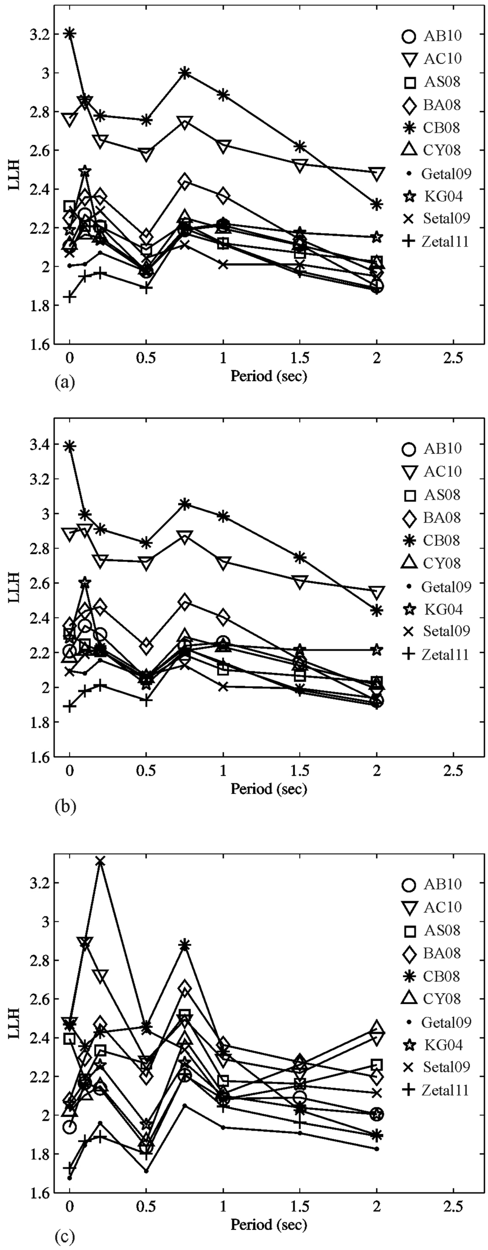

Q9

FIGURE 5 Comparison of LLH values for different ground motion models. (a) all records; (b) record with Mw < 6.25; and (c) records with Mw > 6.25.

8. Ranking of Ground Motion Models by using the Information-Theory Method

The average sample log likelihood (LLH) was calculated for each of the considered periods, using Eq. (3). Figure 5 compares the LLH value for the candidate ground motion models

TABLE 5 Ranking of models based on LH method with respect to $S_a(T = 1.0\text{ s})$

Model Name	Rank	MEDLH	σ	MEDNR	σ	MEANNR	σ	STDNR	σ
T = 1.0 s									
Setal09	A	0.48	0.04	0.00	0.13	0.01	0.10	1.07	0.08
Getal09	B	0.36	0.04	0.38	0.16	0.32	0.11	1.23	0.09
KG04	C	0.40	0.05	−0.64	0.15	−0.56	0.10	1.10	0.08
AB10	C	0.37	0.06	0.56	0.16	0.46	0.12	1.27	0.09
Zetal11	C	0.34	0.05	0.21	0.14	0.15	0.12	1.31	0.10
CY08	C	0.32	0.04	0.02	0.25	0.04	0.13	1.41	0.08
AS08	C	0.30	0.05	0.04	0.20	−0.15	0.13	1.35	0.09
AC10	D	0.32	0.04	0.96	0.12	0.91	0.10	1.09	0.07
BA08	D	0.24	0.03	0.17	0.25	0.21	0.14	1.50	0.09
CB08	D	0.22	0.05	−0.88	0.27	−0.84	0.14	1.56	0.10

in different periods. This figure was prepared for all records: records with $Mw < 6.25$ and records with $Mw > 6.25$, separately.

As shown in Fig. 5, it seems that some of ground motion models are more compatible with the observational data for nearly all periods. For more clarification, rankings of the ground motion models according to the mean LLH values are presented in Table 10 for different periods. We emphasize here that the two models, Getal09 and Setal09, are developed just for the response spectra values, excluding the PGA value. Therefore, these two models are excluded from comparisons. A final period- independent ranking can be created by averaging on LLH values of all periods, as shown in Table 11.

By comparing Table 7 with Table 11, the agreement of LH and the information-theory method in ranking of the models is confirmed. The two models, Getal09, and Zetal11, which are located in top levels of the ranking belong to category 1. In contrast, NGA models are consistently in the lower half of table. The rational judgment gained from this result is that using the application of NGA models for Iran, which is a common practice in many hazard analysis projects, may be questionable (particularly, note that CB08 was fully rejected according to LH method). In order to study the probable dependency of results with magnitude, Tables 12 and 13 were prepared in respect to the ground motions with $Mw > 6.25$ and $Mw < 6.26$, respectively. These results again attest to the superior performance of local models, Getal09 and Zetal11, compared with other models.

Although the ranking method presented here appears to be a powerful tool to examine this question, this is not the main goal of this article and would need a more thorough analysis.

The main objective of this article is to find corresponding weights to be used in seismic hazard analysis. According to Eq. (4), the LLH values can be transformed into compatible weights. However, in order to combine the two methods LH and information-theory method, this procedure is undertaken in two steps.

(1) We assign a general weight to three top models as well as for the five bottom models. The criterion for this weighting is the arithmetic average value of LLH values. The arithmetic average value of LLH index for the three top models is equal to 2.05 and for the other 5 models is 2.21. By using Eq. (4), the overall resulted weights are 0.53, and 0.47, respectively.
(2) The resulting weights are now shared between the corresponding models based on Eq. (4).

TABLE 6 Ranking of models based on LH method for different periods

PGA (T = 0.0 s)

Model Name	Rank	MEDLH	σ	MEDNR	σ	MEANNR	σ	STDNR	σ
Zetal11	A	0.45	0.07	−0.20	0.15	−0.09	0.10	1.10	0.07
CY08	C	0.31	0.06	−0.26	0.22	−0.24	0.13	1.40	0.08
AB10	C	0.31	0.04	0.47	0.18	0.38	0.13	1.36	0.08
AS08	C	0.29	0.06	−0.65	0.19	−0.64	0.12	1.33	0.08
KG04	C	0.26	0.05	−0.42	0.18	−0.36	0.13	1.44	0.08
AC10	D	0.30	0.06	1.04	0.15	1.11	0.10	1.07	0.06
BA08	D	0.27	0.04	−0.13	0.19	0.10	0.14	1.56	0.09
CB08	D	0.13	0.04	−1.07	0.21	−1.04	0.15	1.69	0.09
Getal09									
Setal09									

T = 0.1 s

Model Name	Rank	MEDLH	σ	MEDNR	σ	MEANNR	σ	STDNR	σ
Zetal11	A	0.43	0.06	−0.20	0.14	−0.18	0.10	1.06	0.06
Getal09	B	0.39	0.06	−0.04	0.14	−0.05	0.11	1.23	0.08
Setal09	C	0.37	0.07	0.08	0.16	0.27	0.12	1.29	0.08
CY08	C	0.35	0.06	0.06	0.25	0.00	0.13	1.39	0.08
AS08	C	0.33	0.04	−0.34	0.22	−0.36	0.12	1.32	0.08
AB10	C	0.32	0.05	0.60	0.23	0.47	0.13	1.37	0.08
BA08	D	0.25	0.06	0.07	0.24	0.15	0.14	1.56	0.09
AC10	D	0.25	0.06	1.14	0.16	1.10	0.10	1.10	0.06
KG04	D	0.25	0.04	−0.81	0.20	−0.59	0.13	1.46	0.09
CB08	D	0.17	0.03	−0.76	0.25	−0.80	0.15	1.60	0.09

T = 0.2 s

Model Name	Rank	MEDLH	σ	MEDNR	σ	MEANNR	σ	STDNR	σ
Zetal11	B	0.43	0.07	−0.13	0.11	0.00	0.11	1.15	0.07
Setal09	B	0.42	0.06	0.38	0.16	0.49	0.11	1.22	0.06
Getal09	C	0.36	0.07	0.16	0.12	0.25	0.12	1.27	0.07
AS08	C	0.30	0.05	−0.50	0.14	−0.41	0.12	1.30	0.07
AB10	C	0.29	0.05	0.28	0.16	0.40	0.12	1.34	0.07
CY08	C	0.28	0.09	0.07	0.15	0.09	0.13	1.38	0.07
KG04	C	0.28	0.07	−0.17	0.14	0.05	0.13	1.39	0.07
AC10	D	0.32	0.05	0.98	0.13	0.99	0.09	1.05	0.05
BA08	D	0.28	0.07	0.01	0.14	0.24	0.15	1.56	0.08
CB08	D	0.20	0.03	−0.85	0.19	−0.74	0.15	1.60	0.08

T = 0.5 s

Model Name	Rank	MEDLH	σ	MEDNR	σ	MEANNR	σ	STDNR	σ
Zetal11	A	0.45	0.05	−0.09	0.11	−0.02	0.10	1.12	0.07
Getal09	B	0.43	0.08	0.31	0.12	0.32	0.11	1.16	0.07
AB10	B	0.42	0.07	0.28	0.09	0.34	0.11	1.16	0.07
Setal09	B	0.39	0.05	−0.13	0.12	−0.05	0.11	1.16	0.07

(*Continued*)

TABLE 6 (Continued)

T = 0.5 s									
Model Name	Rank	MEDLH	σ	MEDNR	σ	MEANNR	σ	STDNR	σ
KG04	B	0.37	0.05	−0.47	0.18	−0.38	0.11	1.15	0.07
AS08	C	0.36	0.05	−0.53	0.11	−0.43	0.12	1.25	0.07
BA08	C	0.35	0.06	0.07	0.17	0.20	0.13	1.45	0.08
CY08	C	0.35	0.04	−0.10	0.12	−0.06	0.12	1.30	0.07
AC10	D	0.36	0.05	0.90	0.09	0.99	0.10	1.04	0.06
CB08	D	0.21	0.04	−0.96	0.18	−0.91	0.14	1.49	0.08
T = 0.75 s									
Model Name	Rank	MEDLH	σ	MEDNR	σ	MEANNR	σ	STDNR	σ
Setal09	B	0.42	0.05	−0.12	0.18	−0.07	0.11	1.17	0.08
AB10	C	0.42	0.04	0.42	0.10	0.39	0.12	1.25	0.09
Getal09	C	0.39	0.05	0.41	0.11	0.32	0.11	1.25	0.09
Zetal11	C	0.38	0.06	0.22	0.12	0.15	0.12	1.33	0.10
KG04	C	0.37	0.05	−0.51	0.18	−0.45	0.11	1.18	0.08
AS08	C	0.34	0.06	−0.10	0.15	−0.23	0.13	1.38	0.09
CY08	C	0.28	0.04	0.03	0.14	0.00	0.13	1.44	0.09
AC10	D	0.31	0.05	0.98	0.15	0.97	0.11	1.12	0.08
BA08	D	0.24	0.05	0.28	0.18	0.26	0.14	1.54	0.09
CB08	D	0.21	0.04	−0.92	0.20	−0.87	0.15	1.61	0.10
T = 1.5 s									
Model Name	Rank	MEDLH	σ	MEDNR	σ	MEANNR	σ	STDNR	Σ
Setal09	A	0.49	0.05	0.01	0.12	0.00	0.09	1.00	0.08
Getal09	B	0.48	0.05	0.05	0.09	0.01	0.11	1.15	0.09
Zetal11	B	0.45	0.06	0.15	0.11	0.11	0.11	1.14	0.09
KG04	C	0.39	0.04	−0.61	0.13	−0.49	0.10	1.14	0.08
AB10	C	0.39	0.04	0.56	0.13	0.43	0.11	1.24	0.10
AS08	C	0.36	0.05	0.12	0.13	0.05	0.13	1.34	0.09
BA08	C	0.33	0.06	0.15	0.17	0.11	0.13	1.38	0.09
CY08	C	0.29	0.06	0.27	0.20	0.19	0.13	1.35	0.09
CB08	C	0.27	0.06	−0.64	0.20	−0.72	0.14	1.48	0.10
AC10	D	0.39	0.05	0.82	0.10	0.88	0.10	1.03	0.08
T = 2.0 s									
Model Name	Rank	MEDLH	σ	MEDNR	σ	MEANNR	σ	STDNR	σ
Setal09	A	0.52	0.03	0.03	0.14	−0.08	0.09	1.00	0.07
Zetal11	B	0.45	0.04	0.16	0.09	0.16	0.10	1.13	0.08
Getal09	B	0.44	0.03	0.26	0.14	0.24	0.10	1.04	0.08
AB10	B	0.40	0.05	0.34	0.10	0.32	0.11	1.12	0.08
CY08	B	0.31	0.06	0.26	0.13	0.35	0.12	1.25	0.08
KG04	C	0.42	0.05	−0.56	0.14	−0.56	0.10	1.05	0.07
BA08	C	0.37	0.06	0.00	0.16	0.10	0.12	1.27	0.08
AS08	C	0.36	0.05	0.35	0.19	0.25	0.12	1.30	0.10
CB08	C	0.30	0.04	−0.71	0.18	−0.62	0.13	1.38	0.08
AC10	D	0.37	0.05	0.85	0.11	0.92	0.09	0.98	0.07

TABLE 7 Final ranking of models based on LH method for united residuals, all events

Model name	Rank	MEDLH	σ	MEDNR	σ	MEANNR	σ	STDNR	Σ
All periods, all events									
Setal09	B	0.44	0.02	−0.01	0.05	0.06	0.04	1.17	0.03
Zetal11	B	0.42	0.02	0.03	0.04	0.04	0.04	1.17	0.03
Getal09	B	0.40	0.02	0.16	0.05	0.13	0.04	1.21	0.03
AB10	C	0.37	0.02	0.39	0.05	0.40	0.04	1.26	0.03
KG04	C	0.34	0.02	−0.52	0.07	−0.42	0.04	1.26	0.03
AS08	C	0.33	0.02	−0.22	0.07	−0.24	0.04	1.34	0.03
CY08	C	0.31	0.02	0.03	0.06	0.05	0.05	1.37	0.03
BA08	C	0.28	0.02	0.05	0.07	0.17	0.05	1.48	0.03
AC10	D	0.32	0.02	0.96	0.04	0.98	0.04	1.06	0.02
CB08	D	0.21	0.02	−0.86	0.08	−0.82	0.05	1.55	0.03

TABLE 8 Final ranking of models based on LH method, for events with Mw > 6.25

Model name	Rank	MEDLH	σ	MEDNR	σ	MEANNR	σ	STDNR	σ
All periods, Events with Mw > 6.25									
Zetal11	A	0.53	0.05	−0.03	0.10	−0.24	0.08	1.05	0.06
Getal09	A	0.49	0.05	0.16	0.12	−0.06	0.08	1.04	0.06
KG04	B	0.45	0.04	−0.04	0.11	−0.17	0.10	1.14	0.06
AB10	B	0.41	0.04	0.41	0.12	0.21	0.09	1.11	0.07
CY08	C	0.43	0.04	0.17	0.14	0.04	0.11	1.32	0.08
AS08	C	0.41	0.07	−0.30	0.15	−0.47	0.11	1.38	0.08
Setal09	C	0.39	0.04	0.62	0.11	0.54	0.09	1.07	0.06
CB08	C	0.39	0.06	−0.35	0.17	−0.59	0.12	1.38	0.08
BA08	C	0.37	0.05	0.42	0.13	0.13	0.11	1.32	0.08
AC10	D	0.32	0.03	0.91	0.09	0.72	0.08	0.93	0.06

TABLE 9 Final ranking of models based on LH method, for events with Mw < 6.25

Model name	Rank	MEDLH	σ	MEDNR	σ	MEANNR	σ	STDNR	σ
All periods, Events with Mw < 6.25									
Setal09	B	0.46	0.02	−0.13	0.05	−0.03	0.04	1.16	0.03
Zetal11	B	0.40	0.03	0.06	0.05	0.09	0.04	1.19	0.03
Getal09	B	0.39	0.02	0.16	0.06	0.16	0.04	1.24	0.03
AB10	C	0.36	0.02	0.39	0.06	0.43	0.05	1.29	0.03
AS08	C	0.33	0.02	−0.19	0.07	−0.19	0.05	1.33	0.03
KG04	C	0.32	0.02	−0.61	0.06	−0.46	0.05	1.27	0.03
CY08	C	0.29	0.02	0.00	0.07	0.05	0.05	1.38	0.03
AC10	D	0.32	0.02	0.97	0.05	1.03	0.04	1.07	0.02
BA08	D	0.27	0.02	0.00	0.06	0.18	0.05	1.50	0.03
CB08	D	0.18	0.02	−0.99	0.08	−0.86	0.06	1.58	0.04

TABLE 10 Ranking of models based on information-theoretic method for different periods

PGA (T = 0.0 s)			T = 0.1 s			T = 0.2 s		
Rank	LLH	Model	Rank	LLH	Model	Rank	LLH	Model
1	1.84	Zetal11	1	1.95	Zetal11	1	1.97	Zetal11
2	2.10	AB10	2	2.01	Getal09	2	2.07	Getal09
3	2.11	CY08	3	2.17	CY08	3	2.14	KG04
4	2.19	KG04	4	2.21	AS08	4	2.15	CY08
5	2.25	BA08	5	2.23	Setal09	5	2.21	AB10
6	2.31	AS08	6	2.27	AB10	6	2.21	AS08
7	2.77	AC10	7	2.36	BA08	7	2.29	Setal09
8	3.20	CB08	8	2.49	KG04	8	2.36	BA08
9	—	Zetal11	9	2.85	AC10	9	2.65	AC10
10	—	Getal09	10	2.86	CB08	10	2.78	CB08
T = 0.5 s			T = 0.75 s			T = 1.0 s		
Rank	LLH	Model	Rank	LLH	Model	Rank	LLH	Model
1	1.89	Zetal11	1	2.11	Setal09	1	2.01	Setal09
2	1.97	Getal09	2	2.17	Getal09	2	2.11	Getal09
3	1.98	AB10	3	2.19	AB10	3	2.12	Zetal11
4	1.98	KG04	4	2.19	KG04	4	2.12	AS08
5	1.99	CY08	5	2.20	Zetal11	5	2.20	CY08
6	2.04	Setal09	6	2.22	AS08	6	2.21	AB10
7	2.09	AS08	7	2.25	CY08	7	2.22	KG04
8	2.15	BA08	8	2.44	BA08	8	2.37	BA08
9	2.59	AC10	9	2.75	AC10	9	2.63	AC10
10	2.76	CB08	10	3.00	CB08	10	2.89	CB08
T = 1.5 s			T = 2.0 s					
Rank	LLH	Model	Rank	LLH	Model			
1	1.96	Getal09	1	1.88	Getal09			
2	1.97	Zetal11	2	1.89	Zetal11			
3	2.01	Setal09	3	1.90	AB10			
4	2.07	AS08	4	1.95	Setal09			
5	2.11	CY08	5	1.97	BA08			
6	2.11	AB10	6	2.01	CY08			
7	2.14	BA08	7	2.02	AS08			
8	2.17	KG04	8	2.15	KG04			
9	2.53	AC10	9	2.32	CB08			
10	2.62	CB08	10	2.49	AC10			

The final result of weighting calculations is shown in Fig. 6. It is worth emphasizing Q4 that the proposed logic tree provides just an offer and never takes the place of the expert judgment. In other words, the quantitative values of each branch obtained through the above procedure could be considered as a numerical guide for subjective weighting by experts.

TABLE 11 Final ranking of models based on information-theoretic method for all periods, all events

All periods, all Events		
Rank	LLH	Model
1	1.98	Zetal11
2	2.03	Getal09
3	2.09	Setal09
4	2.12	AB10
5	2.12	CY08
6	2.16	AS08
7	2.19	KG04
8	2.25	BA08
9	2.66	AC10
10	2.80	CB08

TABLE 12 Final ranking of models based on information-theoretic method for all periods, events with Mw > 6.25

All periods, Events Mw > 6.25		
Rank	LLH	Model
1	1.76	Getal09
2	1.78	Zetal11
3	1.82	AB10
4	1.88	KG04
5	1.90	CY08
6	1.92	BA08
7	2.15	AC10
8	2.16	Setal09
9	2.19	CB08
10	2.19	AS08

Using this approach, the uncertainty arising from differences in expert opinions can be decreased. It should be noted that since the major source of uncertainty in the probabilistic seismic hazard analysis originates from ground motion models, any quantitative framework of obtaining weights of logic tree is of great value.

9. Conclusions

Two different approaches were used here to evaluate candidate ground motion models for the Zagros region of Iran. First, by using a set of recorded ground motion data, the computed residuals with respect to different ground motion models were analyzed by using the LH method. Based on this method, two models were unacceptable and the remaining models were ranked as B or C. Second, information theory was employed to rank the

TABLE 13 Final ranking of models based on information-theoretic method for all periods, events with Mw < 6.25

All periods, Events Mw < 6.25		
Rank	LLH	Model
1	2.01	Zetal11
2	2.07	Getal09
3	2.08	Setal09
4	2.15	AS08
5	2.16	CY08
6	2.18	AB10
7	2.25	KG04
8	2.32	BA08
9	2.75	AC10
10	2.92	CB08

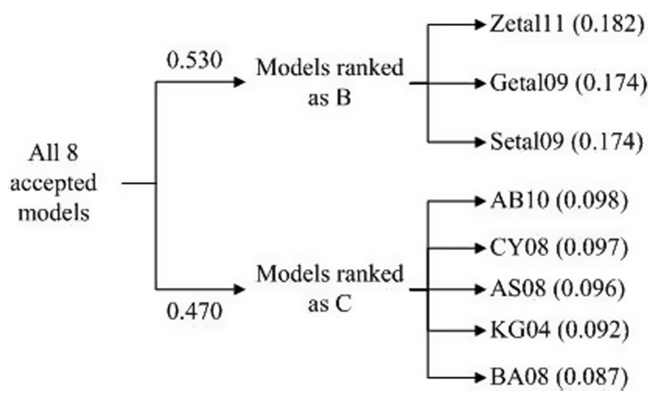

Q9

FIGURE 6 Final weighting results based on combination of LH and information-theory methods.

models, again. The good agreement of these two methods confirms the reliability of the final ranking. One of most significant results of this study was that the regional ground motion models show more consistency with observed data than do models developed using NGA models. Finally, from a combination of the two methods, coherent weights can be calculated that provide a quantitative alternative to expert opinions in seismic hazard projects. These weights can be used to complement expert opinions, where these may be available, or replace expert opinions when these are unavailable. Due to a paucity of data, the testing of the method developed here does not include data from earthquakes with Mw > 6.5 and R < 50 km.

References

Abrahamson, N. and Silva, W. [2008] "Summary of the Abrahamson & Silva NGA ground motion relations," *Earthquake Spectra* **24**(1), 67–97.

Abrahamson, N., Atkinson, G., Boore, D., Bozorgnia, Y., Campbell, K., Chiou, B., Idriss, I.M., Silva, W., and Youngs, R. [2008] "Comparisons of the NGA ground-motion relations," *Earthquake Spectra* **24**(1), 45–66.

Akkar, S. and Bommer, J. J. [2010]. "Empirical equations for the prediction of PGA, PGV and spectral accelerations in Europe, the Mediterranean Region and the Middle East," *Seismological Research Letters* **81**(2), 195–206.

Akkar, S. and Cagnan, Z. [2010] "A local ground-motion predictive model for Turkey, and its comparison with other regional and global ground-motion models," *Bulletin of the Seismological Society of America* **100**, 2978–2995.

Ambraseys, N. N., Douglas, J., Sarma, S. K., and Smit, P. M. [2005]. "Equations for the estimation of strong ground motions from shallow crustal earthquakes using data from Europe and the Middle East: Horizontal peak ground acceleration and spectral acceleration," *Bulletin of Earthquake Engineering* **3**, 1–53.

Ambraseys, N. and Melville, C. [1982] *A History of Persian Earthquakes*, Cambridge University Press, Cambridge.

Ansari, A., Noorzad, As., Zafarani, H., and Vahidifard, H. [2010] "Correction of highly noisy strong motion records using a modified wavelet de-noising method," *Soil Dynamics and Earthquake Engineering* **30**(11), 1168–1181.

Berberian, M. [1995] "Master "blind" thrust faults hidden under the Zagros folds: active basement tectonics and surface morphotectonics," *Tectonophy* **241**, 193–224.

Berberian, M. [1976] "Contribution to the seismotectonics of Iran (Part 2)," *Geological Survey of Iran*, Report 39.

Bommer, J. J., Douglas, J., Scherbaum, F., Cotton, F., Bungum, H., and Fäh, D. [2010] "On the selection of ground-motion prediction equations for seismic hazard analysis," *Seismological Research Letters* **81**, 783–793.

Bommer, J. J. and Scherbaum, F. [2008] "The use and misuse of logic-trees in probabilistic seismic hazard analysis," *Earthquake Spectra* **24**, 997–1009.

Boore, D. and Atkinson, G. [2008] "Ground motion prediction equations for the average horizontal component of PGA, PGV, and 5%-damped PSA at spectral periods between 0.01 s and 10.0 s," *Earthquake Spectra* **24**(1), 99–138.

Budnitz, R. J., Apostolakis, G., Boore, D. M., Cluff, L. S., Coppersmith, K., Cornell, C. A., and Morris, B. J. [1997] "Recommendations for probabilistic seismic hazard analysis, in Guidance on Uncertainty and Use of Experts," Lawrence Livermore National Laboratory, Vol. 2. Q5

Campbell, K. and Bozorgnia, Y. [2008]. "NGA ground motion model for the geometric mean horizontal component of PGA, PGV, PGD and 5%-damped linear elastic response spectra for periods ranging from 0.01 to 10 s," *Earthquake Spectra* **24**(1), 139–171.

Chen S. Z. and Atkinson, G. M. [2002]. "Global comparisons of earthquake source spectra," *Bulletin of the Seismological Society of America* **92**, 885–895.

Chiou, B. S. and Youngs, R. R. [2008]. "An NGA model for the average horizontal component of peak ground motion and response spectra," *Earthquake Spectra* **24**(1), 173–215.

Cotton, F., Pousse, G. F., Bonilla, L., and Scherbaum, F. [2008] "On the discrepancy of recent European ground-motion observations and predictions from empirical models: Analysis of KiK-net accelerometric data and point-sources stochastic simulations," *Bulletin of the Seismological Society of America* **98**, 2244–2261.

Delavaud, E., Scherbaum, F., Kuehn, N., and Riggelsen, C. [2009] "Information-theoretic selection of ground-motion prediction equations for seismic hazard analysis: An applicability study using Californian data," *Bulletin of the Seismological Society of America* **99**, 3248–3263.

Efron, B. and Tibshirani, R. J. [1993] *An Introduction to the Bootstrap*, Chapman & Hall/CRC, New York.

Ghasemi, H., Zare, M., Fukushima, Y., and Koketsu, K. [2009] "An empirical spectral ground-motion model for Iran," *Journal of Seismology*. Q6

Hassani, B., Zafarani, H., Farjoodi, J., and Ansari, A. [2011] "Estimation of site amplification, attenuation and source spectra of S-Waves in the East-Central Iran," *Soil Dynamics and Earthquake Engineering* **31**, 1397–1413.

Hamzehloo, H. [2005] "Determination of causative fault parameters for some recent Iranian earthquakes using near field SH-wave data," *Journal of Asian Earthquake Science* **25**, 621–628.

Hatzfeld, D., Tatar, M., Priestley, K., and Ghafory-Ashtiany, M. [2003] "Seismological constraints on the crustal structure beneath the Zagros Mountain belt (Iran)," *Geophysical Journal International* **155**, 403–410.

Kalkan, E. and Gülkan, P. [2004]. "Site-dependent spectra derived from ground motion records in Turkey," *Earthquake Spectra* **20**(4), 1111–1138.

Krinitzsky, E. L. [1995] "Problems with logic trees in earthquake hazard evaluation," *Engineering Geology* **39**, 1–3.

Montgomery, C. D. and Runger, C. G. [2003] *Applied Statistics and Probability for Engineers*, John Wiley & Sons, Inc., New York.

Nissen, E., Ghorashi, M., Jackson, J., Parsons, B., and Talebian, M. [2007] "The 2005 Qeshm Island earthquake (Iran)-alink between buried reverse faulting and surface folding in the Zagros simply folded belt?," *Geophysical Journal International* **171**, 326–338.

Peyret, M., Rolandone, F., Dominguez, S., Djamour, Y., and Meyer, B. [2008] "Source model for the Mw 6.1, 31 March 2006, Chalan-Chulan Earthquake (Iran) from InSAR," *Terra Nova* **20**, 126–133.

Power, M., Chiou, B., Abrahamson, N., Bozorgnia, Y., Shantz, T., and Roblee, C. [2008] "An Overview of the NGA Project," *Earthquake Spectra* **24**(1), 3–21.

Scherbaum, F., Delavaud, E., and Riggelsen, C. [2009] "a," *Bulletin of the Seismological Society of America* **99**, 3234–3247.

Scherbaum, F., Cotton, F., and Smit, P. [2004] "On the use of response spectral-reference data for the selection of ground-motion models for seismic hazard analysis: The case of rock motion," *Bulletin of the Seismological Society of America* **94**(6), 341–348.

Sharma, M. [2009] "Ground-motion prediction equations based on data from the Himalayan and Zagros regions," *Journal of Earthquake Engineering* **13**(8), 1191–1210.

Toro, G. [2006] "The effects of ground-motion uncertainty on seismic hazard results: Examples and approximate results," *Annual Meeting of the Seismo Seismological Society of America*, San Francisco, California.

Trifunac, M. D. and Lee, V. W. [1973] "Routine computer processing of strong motion accelerograms," Report EERL 73-03, Calif. Inst. of Tech., Pasadena, California.

Zafarani, H., Mousavi, M., Noorzad, A., and Ansari, A. [2008] "Calibration of the specific barrier model to Iranian plateau earthquakes and development of physically based attenuation relationships for Iran," *Soil Dynamics and Earthquake Engineering* **28**, 550–576.

Zafarani *et al*. [2011] "Simulation of ground motion in the Zagros region, Iran using the specific barrier model and stochastic method," *Bulletin of the Seismological Society of America*. Q7

Zafarani *et al*. [2012] Site response and source spectra of S-waves in the Zagros region, Iran," *Soil Dynamics and Earthquake Engineering*. Q8